

# Raman evidence for atomic correlation between the two constituent tubes in double-walled carbon nanotubes

Wencai Ren,<sup>1</sup> Feng Li,<sup>1</sup> Pingheng Tan,<sup>2</sup> and Hui-Ming Cheng<sup>1,\*</sup><sup>1</sup>Shenyang National Laboratory for Materials Science, Institute of Metal Research, Chinese Academy of Sciences, Shenyang 110016, China<sup>2</sup>State Key Laboratory for Superlattices and Microstructures, Institute of Semiconductors, Chinese Academy of Sciences, Beijing 100083, China

(Received 25 January 2006; published 28 March 2006)

Four well-resolved peaks with very narrow linewidths were found in the  $D$ -band and  $G'$ -band features of double-walled carbon nanotubes (DWNTs). This fact implies the occurrence of additional van Hove singularities (vHSs) in the joint density of states (JDOS) of DWNTs, which is consistent with theoretical calculations. According to their peak frequencies and theoretical analysis, the two outer peaks can be deduced to originate from a strong coupling between the two constituent tubes of commensurate DWNTs and the two inner peaks were curvature-related and assigned to originate from the two tubes with a weak coupling. This observation and elucidation constitute the first Raman evidence for atomic correlation and the resulting electronic structure change of the two constituent tubes in DWNTs. This result opens the possibility of predicting and modifying the electronic properties of DWNTs for their electronic applications.

DOI: [10.1103/PhysRevB.73.115430](https://doi.org/10.1103/PhysRevB.73.115430)

PACS number(s): 61.46.-w, 78.30.Na, 81.05.Uw

## I. INTRODUCTION

Recently, much interest has been generated for double-walled carbon nanotubes (DWNTs),<sup>1-4</sup> because of their special double wall structure and their potential for applications in nanoscale devices. For a single-walled carbon nanotube (SWNT), it was well established that its structure can be uniquely determined by its  $(n, m)$  indices.<sup>5,6</sup> However, a DWNT cannot be determined only by two different  $(n, m)$  combinations, but also by the atomic arrangement of its two constituent tubes, i.e., their relative circumferential rotation angle and their axial translation is an important determining parameter.<sup>7,8</sup> Theoretical calculations for energy bands of DWNTs have concluded that their electronic structures are sensitive to their structural symmetry, that is, the atomic correlation between adjacent nanotubes.<sup>7-10</sup> It is possible to change the electronic structure by changing the relative positions of the inner and outer tubes, which controls the amount of lattice matching<sup>7,8</sup> and interlayer interaction. Therefore, it is quite important to identify the atomic correlation between the two constituent tubes of a DWNT and to determine its electronic structure for electronic applications. However, rare experimental results have so far been reported for the atomic correlation of the two constituent tubes of a DWNT and the resulting influence on its electronic structure.

The atom position and electronic structure of an isolated SWNT can be obtained by scanning tunneling microscopy (STM) and spectroscopy (STS).<sup>5</sup> However, the relative atom position and electronic structure of a DWNT cannot be measured by STM/STS directly, since only the outermost nanotube contributes to the STM image and STS conductance measurements.<sup>7</sup> Raman spectroscopy provides a sensitive probe for electronic structure through the coupling between electrons and phonons in the one-dimensional (1D) system. However, the radial breathing mode (RBM) and  $G$  band relate to the center of the two-dimensional (2D) graphite Brillouin zone ( $\Gamma$  point) and are considered to be based on the single resonance mechanism.<sup>11</sup> Therefore, the RBM and  $G$ -band frequencies of an individual tube are independent of the excitation energy but the Raman signals vanish with the laser being less resonant with the van Hove singularities (vHSs) in the joint density of states (JDOS). In contrast to the RBM and  $G$  band, both  $D$ -band and  $G'$ -band features relate to the corner of the 2D graphite Brillouin zone ( $K$  point) and are highly dispersive, showing a strong dependence of their frequencies on the laser excitation energy for SWNT bundles.<sup>6,11</sup> The physical origin of the  $D$ -band and  $G'$ -band features in Raman spectra of isolated tubes is based on the double resonance mechanism, which involves a resonance not only with the incident or scattered photons, but also with an intermediate intraband scattering process.<sup>11,12</sup> According to the double resonance effect, the phonon  $q$  responsible for the  $D$ -band and  $G'$ -band frequencies is strongly related to the resonance electron  $k$  vector. For the nanotubes, the vHSs for the electronic states  $E_{ii}$  will strongly constrain the  $k$  vector and consequently affect the selection of  $q$  vectors involved in the double resonance process.<sup>13,14</sup> Therefore, both the  $D$ -band and  $G'$ -band features are very sensitive to the electronic structure of the nanotubes.

In the present paper, we try to provide Raman evidence for the atomic correlation and the resulting influence on the electronic structures of the two constituent tubes of a DWNT from the resonant Raman profiles of their  $D$ -band and  $G'$ -band spectra. Four well-resolved peaks with very narrow linewidths were found in the  $D$ -band and  $G'$ -band features of double-walled carbon nanotubes (DWNTs). This implies the occurrence of additional vHSs in the JDOS of DWNTs, which is consistent with theoretical calculations. According to their peak frequencies and theoretical analysis, the two outer peaks were deduced to originate from the strong coupling between the two constituent tubes of commensurate DWNTs and the two inner peaks were curvature-related and

lounin zone ( $\Gamma$  point) and are considered to be based on the single resonance mechanism.<sup>11</sup> Therefore, the RBM and  $G$ -band frequencies of an individual tube are independent of the excitation energy but the Raman signals vanish with the laser being less resonant with the van Hove singularities (vHSs) in the joint density of states (JDOS). In contrast to the RBM and  $G$  band, both  $D$ -band and  $G'$ -band features relate to the corner of the 2D graphite Brillouin zone ( $K$  point) and are highly dispersive, showing a strong dependence of their frequencies on the laser excitation energy for SWNT bundles.<sup>6,11</sup> The physical origin of the  $D$ -band and  $G'$ -band features in Raman spectra of isolated tubes is based on the double resonance mechanism, which involves a resonance not only with the incident or scattered photons, but also with an intermediate intraband scattering process.<sup>11,12</sup> According to the double resonance effect, the phonon  $q$  responsible for the  $D$ -band and  $G'$ -band frequencies is strongly related to the resonance electron  $k$  vector. For the nanotubes, the vHSs for the electronic states  $E_{ii}$  will strongly constrain the  $k$  vector and consequently affect the selection of  $q$  vectors involved in the double resonance process.<sup>13,14</sup> Therefore, both the  $D$ -band and  $G'$ -band features are very sensitive to the electronic structure of the nanotubes.

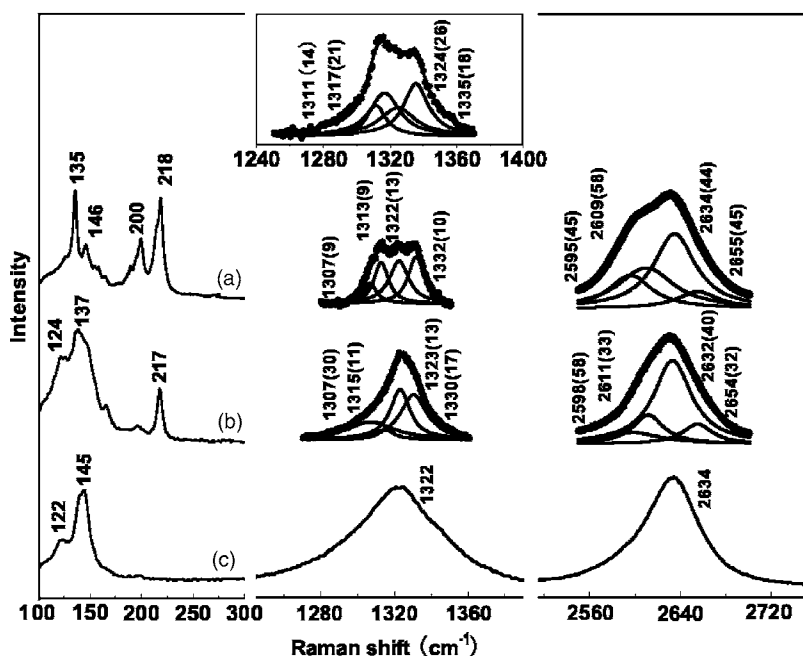


FIG. 1. Raman spectra of the RBM, *D* band and *G'* band measured with a laser energy of 1.96 eV of (a) sample containing more than 90% DWNTs with outer and inner diameter of  $1.85 \pm 0.15$  and  $1.15 \pm 0.15$  nm, respectively, (b) sample containing about 30% DWNTs and 70% SWNTs with the similar outer diameter of 1.85 nm, and (c) SWNTs with average diameter of 1.85 nm. The inset shows a fit to the *D* band of DWNTs with a larger diameter of 2.26 nm. A Lorentzian line shape was used in the fitting process. The frequencies/widths of the observed modes are also displayed.

originated from the two tubes with weak coupling.

## II. EXPERIMENT

Three DWNT samples with different diameter distributions were used in this study and were prepared by a floating catalytic decomposition of methane with different amounts of sulfur addition.<sup>2,15,16</sup> The first sample consisted of aligned DWNT ropes (more than 90% DWNTs in the sample) with outer and inner diameters of  $1.85 \pm 0.15$  and  $1.15 \pm 0.15$  nm, respectively.<sup>15</sup> A great deal of HRTEM observations showed that the mean outer and inner diameter of the other sample (more than 70% DWNTs) are 2.26 nm and 1.52 nm, respectively.<sup>2</sup> Another sample, containing about 30% DWNTs, was also synthesized by the floating catalyst method and their average outer and inner tube diameters are 1.85 and 1.15 nm, respectively. Moreover, it should be pointed out that: (1) no multiwalled carbon nanotubes (MWNTs) were found in the above samples, and (2) the rest of the samples, except for DWNTs, consisted of SWNTs with a diameter similar to the outer diameter of the DWNTs. The large and small diameter SWNTs (average diameter 1.85 nm and 1.20 nm, respectively) used for comparative experiments were synthesized by the floating catalytic decomposition of methane and ethanol chemical vapor deposition (CVD), respectively.<sup>16</sup> All the above structural information of the samples studied was obtained from a great deal of HRTEM observations. Resonant Raman measurements were performed in the backscattering configuration at room temperature using three laser energies ( $E_{\text{laser}}$ ) of 1.96, 2.41, and 2.54 eV. We fitted the *D*-band and *G'*-band features using a sum of Lorentzians.

## III. RESULTS AND DISCUSSION

Figure 1 shows the *D*-band and *G'*-band Raman features of different samples measured with the 1.96 eV laser excita-

tion, in which Fig. 1(a) is from the DWNT rope with a narrow diameter distribution, Fig. 1(b) is from the sample containing about 30% DWNTs, and Fig. 1(c) from the SWNTs with an average diameter of 1.85 nm. It is clear that the *D* band and *G'* band of the samples containing DWNTs are composed of four well-resolved peaks and those of the SWNTs are a single peak. The inset of Fig. 1 shows the *D* band of DWNTs with a larger outer diameter of 2.26 nm. Note that the four-peak Raman features of the *D* band and *G'* band could be observed in both DWNT samples with different mean diameters, and their frequencies were dependent on the mean nanotube diameter. Moreover, the four peaks can be reproducibly found in the *D* band at the different positions of the sample, as shown in Fig. 2, with the same position and linewidth. Therefore, we conclude that the four components

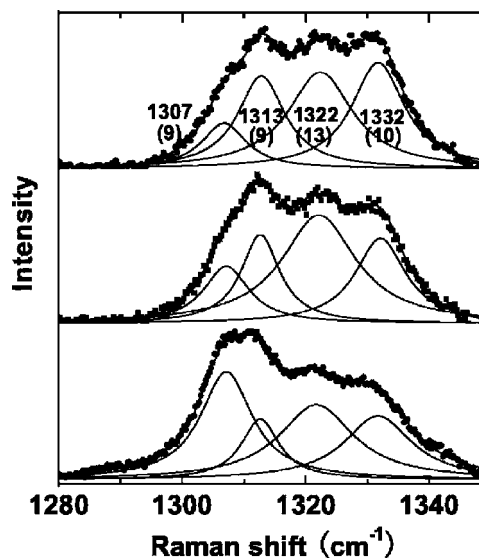


FIG. 2. The reproducible *D*-band feature at different positions of an aligned DWNT rope.

arise from the intrinsic structural features of DWNTs. In the following paragraphs, we will discuss the physical origin of the unique *D*-band and *G'*-band features observed in DWNTs based on double resonance mechanism.

In the case of nanotubes, the presence of vHSs in the JDOS greatly affects the result of double resonant process and the resulting peak structure and position of the *D* band.<sup>15,16</sup> Moreover, according to the double resonance mechanism, not only the quantized electronic structure but also the phonon dispersion relations of the nanotubes should be taken into account to quantitatively analyze the fine structure of the *D* band of nanotubes.<sup>12,17</sup> Zólyomi *et al.*<sup>17</sup> considered that the fine structure of the *D*-band feature for SWNT bundles was dependent on four factors: the triple resonant transitions originating from the vHSs (i.e., the double resonance conditions with the scattering process occurring between electronic states in the *k* space corresponding to vHSs in the density of states), chirality distribution of SWNTs in the sample, the trigonal warping of the phonon dispersion, and the reciprocal lifetime of the excited states. Moreover, it was worth noting that the main peak originates from the SWNTs satisfying the triple resonant condition, and the sidebands of the *D* band with a relative small intensity originate from those SWNTs that are somewhere between being truly triple resonant and merely double resonant. Generally, only a relatively small number of SWNTs have the vHSs satisfying the triple resonance condition in a SWNT sample with a Gaussian diameter distribution. Accordingly, only one main band was observed in the *D* band, with the frequency  $\omega_D$  equal to the weighted average of all the  $\omega_D$  for the SWNTs satisfying the triple resonance conditions.<sup>13</sup>

Damnjanovic *et al.*<sup>18</sup> calculated the phonon dispersion relations of the commensurate DWNTs based on symmetry and found that the high-energy modes are scarcely influenced by the interlayer interaction. This result implies that the unique *D*-band structure of DWNTs should not originate from the change of phonon dispersion relations. In order to elucidate the physical origin of the unique *D*-band feature, first, we assume that the electronic structures of the two constituent tubes of DWNTs are not changed. Based on the above elucidation on the *D*-band feature for SWNT bundles, it is expected to have two main peaks for the *D* band of DWNTs because of the Gaussian diameter distribution of the outer and inner tubes of DWNTs. However, four well-resolved main components were found in the *D* band experimentally, indicating that they should not be a mere consequence of the diameter distribution of the DWNTs.

To further rule out the diameter distribution origin of the four peaks, a comparative experiment was designed, in which a SWNT sample with a large diameter (1.85 nm) similar to the outer tube diameter of the DWNTs was sonicated in ethanol and the dispersed SWNT bundles obtained were dropped onto a Si(100) substrate covered with small diameter SWNTs (1.20 nm) similar to the inner tube diameter of the DWNTs to form a mixture of two kinds of SWNTs with different diameters. Figure 3 shows the RBM and *D* bands of the large diameter SWNTs, small diameter SWNTs and their mixture, respectively. We can see that the *D* band of the mixture is simply superposed by the two *D* bands of the original SWNT samples originating from the curvature effect

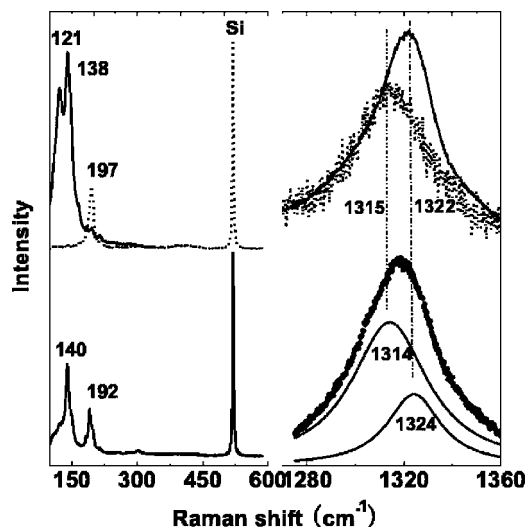


FIG. 3. The RBM and *D* band of (a) two separated SWNTs with average diameters of 1.85 nm and 1.20 nm, respectively, and (b) the mixture of the two SWNTs in (a).

of the nanotubes, without the occurrence of the two additional peaks. Considering that the four additional peaks can even appear in a sample containing only a small amount of DWNTs, as indicated in Fig. 1(b), we can conclude that the four peaks in the *D* band and *G'* band are related to the atomic correlation and the resulting electronic structures of DWNTs.

It is important to note that the four components in the *D* band of DWNTs have comparable intensity and exhibit very small linewidth of about 9–13  $\text{cm}^{-1}$ , comparable to the intrinsic linewidth of a single SWNT.<sup>19</sup> This result indicates that (1) incident and scattered phonons are very close to the vHSs (Ref. 19) (i.e., satisfying the triple resonance condition), and (2) the density of states is very singular, leading to a long phonon lifetime, consistent with the result from RBM analysis,<sup>20</sup> which provide direct evidence for the correlations between the four peaks and the intrinsic electronic structures of DWNTs. Moreover, it was worthy to note that only one main peak was found in the *D*-band feature for an upshift of about 0.2 eV in the  $E_{ii}$  energy transition resulting from the intertube interactions in SWNT bundles.<sup>13</sup> Therefore, we deduce that the occurrence of additional vHSs in the JDOS plays a key role in the unique feature of the *D* band and *G'* band of DWNTs.

Theoretically, the band repulsion can be expected for the energy bands with the same symmetry of wave functions belonging to two different nanotubes due to the large matrix elements of interlayer interaction, leading to the splitting of the energy bands for the two constituents of DWNTs.<sup>7,8</sup> As for the wave functions with different symmetries, the energy bands can cross each other, since the wave functions remain orthogonal to each other even in the presence of interlayer interaction.<sup>7,8</sup> Generally, there are two kinds of DWNTs, commensurate and incommensurate, depending on the ratio of two different lattice constants of the constituents.<sup>7,8</sup> The commensurate cases are the cases of achiral DWNTs, since translation vectors are the same for two armchair nanotubes or for two zigzag nanotubes.<sup>7</sup> For a general chiral DWNT,

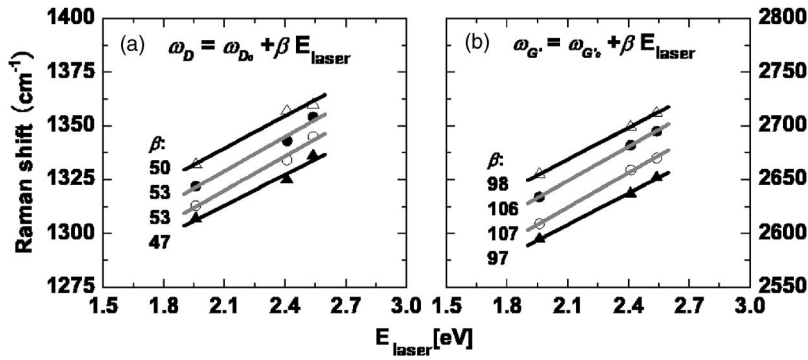


FIG. 4. Laser excitation energy dependence of  $\omega_D$  (a) and  $\omega_{G'}$  (b) for DWNTs with outer and inner diameter of  $1.85 \pm 0.15$  and  $1.15 \pm 0.15$  nm, respectively.

the two constituent tubes are expected to be incommensurate and have only  $2\pi$  rotational symmetry along the chiral vectors which are both perpendicular to the nanotube axis.<sup>8</sup> Thus the energy bands of the inner tube are not degenerated with those of outer tube. Therefore, the electronic property of an incommensurate DWNT can be considered to be the sum of the electronic structures of two independent nanotubes, expect for some small modification due to a weak interlayer interaction. According to our previous researches,<sup>2,15,16</sup> the diameters of inner and outer tubes of DWNTs have a Gaussian distribution, respectively. Therefore, two main peaks could be expected in the  $D$  band of the incommensurate DWNTs, having approximate frequencies with those of independent SWNTs with similar diameters.

Considering the diameter difference of  $\sim 0.7$  nm and their resonance contributions from different vHSs subbands, the spring constant mechanism is dominant in the determination of  $\omega_D$  of the two constituent tubes.<sup>21</sup> Therefore, we can preliminarily estimate their frequencies on the basis of the diameter dependence of the  $D$  band of SWNTs. It is well known that the  $\omega_D$  of SWNTs decreases as their diameter ( $d_t$ ) decreases with a simple linear relation  $\omega_D = \omega_0 - \beta/d_t$ ,<sup>22</sup> attributed to the softening of the spring constant due to the curvature effect of individual SWNTs in bundles,<sup>6</sup> where  $\omega_0$  is the  $D$ -band frequency for 2D graphite. According to the relation between  $\omega_D$  and  $d_t$  for  $E_{\text{laser}} = 1.96$  eV,  $\omega_D = 1331 - 16.5/d_t$ ,<sup>22</sup> the  $\omega_D$  of the outer tube with a mean diameter of about 1.85 nm can be predicted to be  $\sim 1322$   $\text{cm}^{-1}$ , which is in a good agreement with the observed high frequency component of the  $D$  band ( $1322$   $\text{cm}^{-1}$ ). For an average interlayer spacing of 0.37 nm, the  $\omega_D$  of the inner tube should be  $\sim 1316$   $\text{cm}^{-1}$  (corresponding to 1.11 nm), which approaches the observed  $1313$   $\text{cm}^{-1}$ . Therefore, the inner two peaks can be assigned to originate from the incommensurate DWNTs. The obtained  $D$ -band frequency agreement between DWNTs and SWNTs with the similar diameters provides strong evidence for the weak interlayer interaction between the two constituents of the incommensurate DWNTs.

Commensurate DWNTs have a better atomic correlation and a stronger van der Waals interaction between the two constituents than those of incommensurate ones. Two important changes were predicted theoretically for the electronic structures of commensurate DWNTs: (1) occurrence of additional vHSs due to the separation of original degenerated energy bands with the same symmetry, and (2) very singular density of states at many anticrossings of energy bands due to the interlayer interaction.<sup>8</sup> The occurrence of additional

vHSs makes it possible to give rise to some additional vHSs satisfying the triple resonance conditions. Moreover, the very singular density of states makes related  $D$ -band frequencies distinguishable due to the resulting very narrow linewidth. Consequently, some new peaks were expected to appear in the  $D$  band of commensurate DWNTs, having different frequencies with those of incommensurate DWNTs. Therefore, the two observed outer peaks in the  $D$  band can be deduced to originate from the occurrence of additional vHSs related to a stronger interlayer interaction for the commensurate DWNTs in the sample.

It was well known that each  $(n, m)$  SWNT has distinctive vHSs attributed to the electronic trigonal warping effect.<sup>22</sup> However, it is possible to find two vHSs with a wave vector  $k$  of the same magnitude and opposite direction, due to modification of the electronic trigonal warping effect for the commensurate zigzag @ zigzag DWNTs. Thus, the corresponding  $D$ -band frequency splitting is dependent on the phonon trigonal wrapping effect. It is very interesting to find that the observed  $D$ -band frequency difference,  $\Delta\omega_D = 25$   $\text{cm}^{-1}$ , for the two outer peaks is in good agreement with the splitting for the related phonon frequencies between the directions  $KM$  and  $K\Gamma$ ,  $\Delta\omega_{\text{ph}} = 24$   $\text{cm}^{-1}$ .<sup>23</sup> This result provides one possibility to quantitatively explain the frequency splitting of the two outer components in the  $D$  band of DWNTs. Moreover, recent HRTEM studies on DWNTs showed that it was possible to have the atomic correlation as a commensurate graphene stacking with zig-zag chains in some local areas for the circumscribed DWNTs in their bundles with a strong van der Waals interaction between the neighboring layers,<sup>24</sup> which provides experimental evidence for the above analysis.

Recently, Barros *et al.*<sup>25</sup> studied the Raman spectra of graphitic foams, which are composed of two intermixed graphitic structures, one with stacked planes and one with a turbostratic structure. It is interesting to note that the  $G'$  band of graphitic foams is composed of three peaks in the range between 2550 and 2680  $\text{cm}^{-1}$ , one corresponding to the contribution from 2D graphite and two from 3D graphite. This is consistent with the above results observed for the  $D$  band and  $G'$  band profiles of our DWNTs. Figures 4(a) and 4(b) show, respectively, the laser energy dependence of  $\omega_D$  and  $\omega_{G'}$ . It is noteworthy that the inner two components of  $D$  band and  $G'$  band have a stronger  $E_{\text{laser}}$  dependence than the outer ones. The inner two components exhibit a similar  $E_{\text{laser}}$  dependence relation to that observed in SWNTs and 2D graphite,<sup>13,26</sup> having a slope of about 53 and 106  $\text{cm}^{-1}/\text{eV}$ ,

respectively. However, the outer two components exhibit a weaker  $E_{\text{laser}}$  dependence with a slope of about 47 and  $97 \text{ cm}^{-1}/\text{eV}$ , respectively, approaching that for 3D graphite.<sup>27,28</sup> Moreover, it is worth noting that the averages between the frequencies of the two  $D$  bands of commensurate DWNTs are  $1319.5 \text{ cm}^{-1}$ ,  $1341 \text{ cm}^{-1}$ , and  $1348 \text{ cm}^{-1}$  for the 1.96 eV, 2.41 eV, and 2.54 eV excitation, respectively. These values are very close to the averages of  $D$ -band frequencies of incommensurate DWNTs, which are of  $1317.5 \text{ cm}^{-1}$ ,  $1338.5 \text{ cm}^{-1}$ , and  $1349.5 \text{ cm}^{-1}$  for the 1.96 eV, 2.41 eV, and 2.54 eV excitation, respectively. The above results are in good agreement with those obtained from graphitic foams.

The detailed structural information of DWNTs and graphitic foams was taken into account to gain a further insight into the similarity of their Raman features and inherent physical correlations. Note that the incommensurate DWNTs are similar to the turbostratic graphite structure in graphitic foams, i.e., the neighboring layers are not stacked with respect to one another with a good atomic correlation. Therefore, the interlayer interactions between the neighboring layers are weakened, leading them to behave as if they were isolated. However, for commensurate DWNTs, their structures are similar to 3D graphite in graphitic foams, with neighboring layers stacking with a good atomic correlation and a strong interlayer interaction. Therefore, the similarities of Raman features further prove that it is the different atomic correlations and the resulting different interlayer interactions that play a key role in the profiles of  $D$  band and  $G'$  band of carbon materials, such as DWNTs, 3D graphite, turbostatic graphite, and graphitic foams.

According to the assignment of the physical origin of the four peaks in the  $D$  band, a rich  $D$ -band structure can be expected depending on the amount of DWNTs with different structures. Indeed, one, two, three, and four main peaks in the  $D$  band were found experimentally at different positions, as shown in Fig. 5, which also provides support for the above assignment. However, further theoretical studies and investigations on isolated DWNTs are required to justify this deduction.

All the above analyses indicate that atomic correlation between the two constituent tubes of DWNTs plays a very important role in the determination of their  $D$ -band and  $G'$ -band profiles, which is consistent with the results from RBM analysis.<sup>20</sup> To interpret the line splitting in the RBM feature of DWNTs, Pfeiffer *et al.*<sup>20</sup> used the Lennard-Jones (LJ) potential to describe the interlayer interaction and found that the difference in the interaction energy is rather small for the DWNTs with the same inner diameters, due to the small difference in outer diameters. Moreover, it is important to note that the atomic correlation of the two constituents of DWNTs has a stronger influence on the interlayer interaction attributed to their larger contribution to the distance of carbon atoms. However, the interlayer interaction of DWNTs has a larger effect for the lowest frequency modes with radial mode displacements, and much smaller effects for high frequency modes,<sup>18,29</sup> as the effect of intertube interactions in a SWNT bundle.<sup>5</sup> Therefore, the line splitting of the RBM feature of DWNTs is dominantly attributed to the change of phonon dispersion relation resulting from the relative change

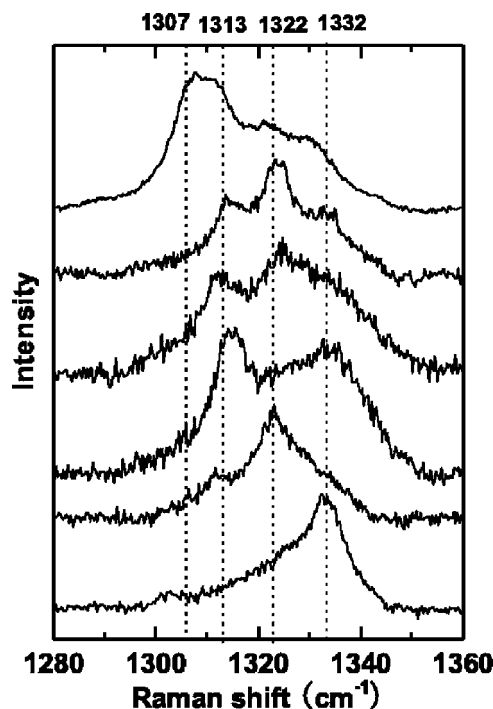


FIG. 5. The  $D$ -band feature obtained at different positions of an aligned DWNT rope.

of the mutual positions of hexagons in the constituent tubes. As we stated above, the line splitting of the  $D$  band was dominantly attributed to the modification of the electronic structure. Therefore, a common conclusion that can be drawn here is that the atomic correlation between the two constituent tubes of a DWNT is an important structural parameter, which has a strong influence on the properties of DWNTs, such as electronic structure and phonon dispersion relation.

#### IV. CONCLUSION

We have made assignment of the four peaks firstly found in the  $D$  band and  $G'$  band of DWNT bundles. The result indicates that the atomic correlation of the two constituent tubes of a DWNT can be probed by studying the spectral profiles of the  $D$  band and  $G'$  band of DWNTs, which cannot be obtained from the RBM and  $G$  band, which only provide information on their  $(n, m)$  configurations. This finding implies that (1) the atomic correlation between the two constituent tubes of DWNTs has a very important influence on their electronic structures, and (2) additional vHSs occur in the JDOS of commensurate DWNTs compared to those of independent SWNTs, which is consistent with theoretical calculations. However, further experimental investigations on isolated DWNTs are required to justify this deduction.

#### ACKNOWLEDGMENTS

The authors acknowledge M. S. Dresselhaus and G. Dresselhaus for constructive discussions, advice, and fruitful comments. This work is supported by NSFC Grants No. 50328204 and No. 90206018.

- \*Author to whom correspondence should be addressed. Electronic address: cheng@imr.ac.cn
- <sup>1</sup>S. Bandow, M. Takizawa, K. Hirahara, M. Yudasaka, and S. Iijima, *Chem. Phys. Lett.* **337**, 48 (2001).
  - <sup>2</sup>W. C. Ren, F. Li, J. Chen, S. Bai, and H. M. Cheng, *Chem. Phys. Lett.* **359**, 196 (2002).
  - <sup>3</sup>S. Okada and A. Oshiyama, *Phys. Rev. Lett.* **91**, 216801 (2003).
  - <sup>4</sup>G. G. Chen, S. Bandow, E. R. Margine, C. Nisoli, A. N. Kolmogorov, V. H. Crespi, R. Gupta, G. U. Sumanasekera, S. Iijima, and P. C. Eklund, *Phys. Rev. Lett.* **90**, 257403 (2003).
  - <sup>5</sup>M. S. Dresselhaus and P. C. Eklund, *Adv. Phys.* **49**, 705 (2000).
  - <sup>6</sup>M. S. Dresselhaus, G. Dresselhaus, A. Jorio, A. G. Souza Filho, and R. Saito, *Carbon* **40**, 2043 (2002).
  - <sup>7</sup>R. Saito, G. Dresselhaus, and M. S. Dresselhaus, *Physical Properties of Carbon Nanotubes* (Imperial College, London, 1998).
  - <sup>8</sup>R. Saito, G. Dresselhaus, and M. S. Dresselhaus, *J. Appl. Phys.* **73**, 494 (1993).
  - <sup>9</sup>Y. K. Kwon and D. Tománek, *Phys. Rev. B* **58**, R16001 (1998).
  - <sup>10</sup>S. Sanvito, Y. K. Kwon, D. Tománek, and C. J. Lambert, *Phys. Rev. Lett.* **84**, 1974 (2000).
  - <sup>11</sup>M. S. Dresselhaus, G. Dresselhaus, R. Saito, and A. Jorio, *Phys. Rep.* **409**, 47 (2005).
  - <sup>12</sup>C. Thomsen and S. Reich, *Phys. Rev. Lett.* **85**, 5214 (2000); R. Saito, A. Jorio, A. G. Souza Filho, G. Dresselhaus, M. S. Dresselhaus, and M. A. Pimenta, *ibid.* **88**, 027401 (2001).
  - <sup>13</sup>A. G. Souza Filho, A. Jorio, G. Dresselhaus, M. S. Dresselhaus, R. Saito, A. K. Swan, M. S. Ünlü, B. B. Goldberg, J. H. Hafner, C. M. Lieber, and M. A. Pimenta, *Phys. Rev. B* **65**, 035404 (2001).
  - <sup>14</sup>J. Kürti, V. Zólyomi, A. Grüneis, and H. Kuzmany, *Phys. Rev. B* **65**, 165433 (2002).
  - <sup>15</sup>W. C. Ren and H. M. Cheng, *J. Phys. Chem. B* **109**, 7169 (2005).
  - <sup>16</sup>W. C. Ren, F. Li, S. Bai, and H. M. Cheng, *J. Nanosci. Nanotech.* (to be published).
  - <sup>17</sup>V. Zólyomi, J. Kürti, A. Grüneis, and H. Kuzmany, *Phys. Rev. Lett.* **90**, 157401 (2003).
  - <sup>18</sup>M. Damnjanović, I. Milošević, E. Dobardžić, T. Vuković, and B. Nikolić, *Phys. Rev. B* **69**, 153401 (2004).
  - <sup>19</sup>A. Jorio, C. Fantini, M. S. S. Dantas, M. A. Pimenta, A. G. Souza Filho, Ge. G. Samsonidze, V. W. Brar, G. Dresselhaus, M. S. Dresselhaus, A. K. Swan, M. S. Ünlü, B. Goldberg, and R. Saito, *Phys. Rev. B* **66**, 115411 (2002).
  - <sup>20</sup>R. Pfeiffer, H. Kuzmany, Ch. Kramberger, Ch. Schaman, T. Pichler, H. Kataura, Y. Achiba, J. Kürti, and V. Zólyomi, *Phys. Rev. Lett.* **90**, 225501 (2003).
  - <sup>21</sup>A. G. Souza Filho, A. Jorio, Ge. G. Samsonidze, G. Dresselhaus, M. A. Pimenta, M. S. Dresselhaus, A. K. Swan, M. S. Ünlü, B. B. Goldberg, and R. Saito, *Phys. Rev. B* **67**, 035427 (2003).
  - <sup>22</sup>R. Saito, G. Dresselhaus, and M. S. Dresselhaus, *Phys. Rev. B* **61**, 2981 (2000).
  - <sup>23</sup>Ge. G. Samsonidze, R. Saito, A. Jorio, A. G. Souza Filho, A. Grüneis, M. A. Pimenta, G. Dresselhaus, and M. S. Dresselhaus, *Phys. Rev. Lett.* **90**, 027403 (2003).
  - <sup>24</sup>A. Hashimoto, K. Suenaga, K. Urita, T. Shimada, T. Sugai, S. Bandow, H. Shinohara, and S. Iijima, *Phys. Rev. Lett.* **94**, 045504 (2005).
  - <sup>25</sup>E. B. Barros, N. S. Demir, A. G. Souza Filho, J. Mendes Filho, A. Jorio, G. Dresselhaus, and M. S. Dresselhaus, *Phys. Rev. B* **71**, 165422 (2005).
  - <sup>26</sup>L. G. Cancado, M. A. Pimenta, R. Saito, A. Jorio, L. O. Ladeira, A. Grüneis, A. G. Souza-Filho, G. Dresselhaus, and M. S. Dresselhaus, *Phys. Rev. B* **66**, 035415 (2002).
  - <sup>27</sup>P. H. Tan, Y. M. Deng, and Q. Zhao, *Phys. Rev. B* **58**, 5435 (1998).
  - <sup>28</sup>M. J. Matthews, M. A. Pimenta, G. Dresselhaus, M. S. Dresselhaus, and M. Endo, *Phys. Rev. B* **59**, R6585 (1999).
  - <sup>29</sup>V. N. Popov and L. Henrard, *Phys. Rev. B* **65**, 235415 (2002).